

USING PCA AND ANN IN THE EXPLANATION OF GROUNDWATER CHEMISM. CASE OF THE MESSAAD PLATEAU. SOUTH ALGERIAN STEPPE REGION

B. E. Rahmani*, F. Baali and C. Fehdi

Water and Environment Laboratory, Faculty of Exact Sciences and Natural and Life Sciences,
University of Tébessa, 12000 Tébessa, Algeria

Received: 21 August 2020 / Accepted: 17 September 2021 / Published online: 01 January 2022

ABSTRACT

The objective of this work is to study the chemistry of groundwater in the messaad plateau which is located 300km south of the capital of Algiers. The results obtained showed that the waters are very strongly mineralized overall, with a predominance of calcium sulphate facies and calcium chloride facies. a high degree of mineralization in the South and South-East part of the study area near Oued Messaad. The Principal Component Analysis (PCA) has shown that the increase in mineralization is mainly due to the dissolution of evaporative mineral-rich salt-bearing formations. The hydro-chemical model based on Artificial Neuron Networks (ANN) of the multilayer perceptron (MLP) type has shown that the SO_4^{2-} , Cl^- , Ca^{2+} , Na^+ ions are the most important factors influencing the electrical conductivity of water. These ions are the result of the dissolution of gypsum and halite continuously in the clays and marls of the Barremian formations.

Keywords: Barremian formations; evaporative; Mineralization; Oued Messaad; Algeria.

Author Correspondence, e-mail: Afrmlk@gmail.com

doi: <http://dx.doi.org/10.4314/jfas.v14i1.5>



1. INTRODUCTION

The area studied (messaad plateau) is part of the arid zones of Algeria. It is located 370 km south of the capital Algiers. The studied area is characterized by its agricultural and agropastoral vocation. Currently agriculture is booming in the region, these agricultural and agropastoral activities therefore require water resources, which will be able to meet the needs of the region, with a view to achieving sustainable development of the study area. So under these conditions and in the absence of surface water resources, the barremian, which is the main aquifer in the region, is the most sought after by the rural population in all the steppe areas of the region. It is exploited by wells of large diameters and boreholes.

The high demand for irrigation water and even drinking water in the study region will accentuate the constraints on this resource. In addition, natural factors, such as geological constraints, have an effect on the quality of groundwater. Pollution can also play a role in the degradation of water quality, because the wastewater from domestic sources discharged directly into the Oued Messaad which crosses the city from west to east, these waters can infiltrate and pollute the water table [9]. Previous hydrogeological work on this area is scarce and does not discuss the quality of groundwater [10,11], but consultation of the results of the physical analyses Water chemistry of some wells, carried out by the ANRH (Agence Nationale des Ressources Hydraulique), shows important values of the chemical elements exceeding the standards set by the WHO (World Health Organization), with conductivity values exceeding 2000 $\mu\text{S}/\text{cm}$, These values show a deterioration in groundwater quality, so it is essential to quantify and analyze the quality of the water supply and how to manage this resource to ensure sustainability. The present study is intended to characterize the physico-chemical quality of groundwater and to explain of groundwater chemism using PCA and ANN methods.

2. MATERIALS AND METHODS

2.1. Presentation of the study area

The Messaad Plateau which covers an area of 950 km² is located 370 Km South of the capital of Algiers, it is located about 75 km south East of Djelfa city, and 60 Km North of the Wilaya of Laghouat, Limited by longitudes 3°13'0.3020'' and 3°39'8.3384'' and latitudes 34°4'23.0794'' and 34°20'31.5612''. Surrounded by the massifs of the Djebels: Mergueb, zerga, Tafara and BouKahil (Fig. 01), the altitudes vary from 600 to 1460 m.

The plateau belongs mainly to the West of the large basin chott Melghigh coded 06, more exactly, in the swallowed part of the subwatershed of the Oued Demmede coded 06-06.

The remoteness of the study area from the sea (about 370 km) and its position in the southern part of the Central Saharan Atlas, gives it an arid continental climate, characterized by a cold winter with annual precipitation of the order of 150 mm. The year-to-year average temperature is 19.23°C.

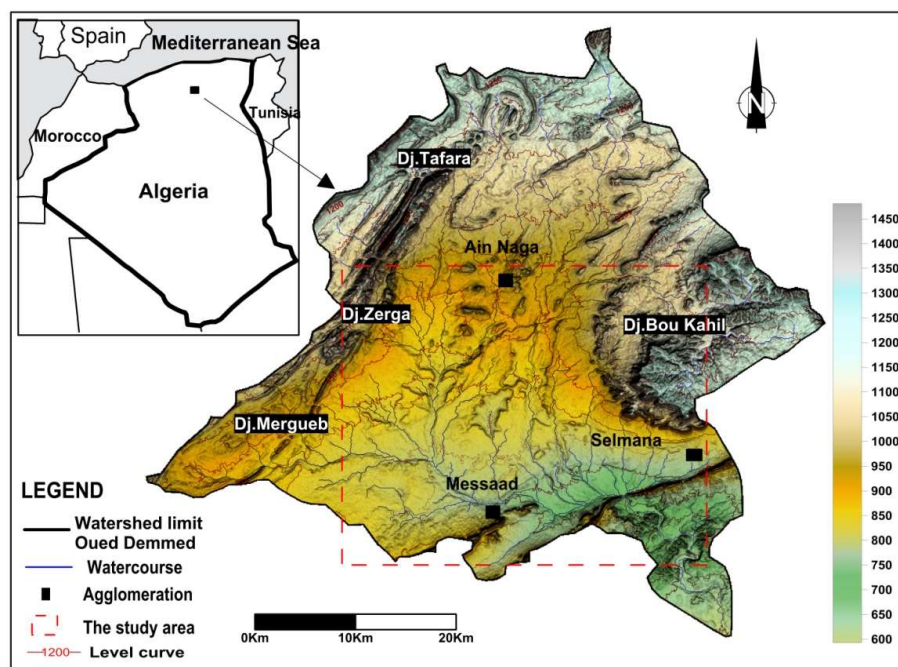


Fig.1. Study area situation.

2.2. Geology and hydrogeology

The basin area of the Oued Demmede consisting of a material of continental age, Jurassic, Cretaceous, Tertiary and Quaternary nature [2,16]. These are essentially Superficial formations that are little or no tectonised, detritical The formations of the Jurassic and Cretaceous where alternate series mainly hard limestone more or less dolomitic, with predominantly soft marl-limestone alternating with marls, predominantly sandstone with intercalations of versicolores gypsus and more or less salty clays.

In the Messaad region, the Barremian aquifer forms the main source of water supply for drinking water and irrigation water with primary permeability and cracks with a thickness ranging from 250 to 300 m [11], is mainly sandstone and clay sandstone [17]. Its position in synclinal is a great advantage and the majority of drill holes capture this aquifer, their operating flows vary, it is strong in the West zone and weak in the East zone [10]. The

presence of past gypsum and marl clays in sandstone divides the Barremian aquifer layer into several isolated aquifers. The supply of water is made directly from the precipitation or indirectly from the massifs of the Djebels: Mergueb, and Zerga, by runoff or by infiltration through faults, with a main groundwater flow direction (NW-SE) as shown in the piezometric map of July 2018 (Fig 02).

We also find the MPQ layer which forms a secondary source and which it excites only in certain parts of the study area, constituted by an alternation of sandy clay of gravel sandstone and conglomerate, the latter are based in discordance on the Barremian formations [2,16].

In recent years, the Messaad region has suffered from poor groundwater quality and is deteriorating its quality due to a number of reasons; including natural factors such as drought or lithology, have an effect on water quality. In addition, anthropogenic activities can play a role in the degradation of water quality. In order to explain the chemistry of these waters, we used statistical methods in our study.

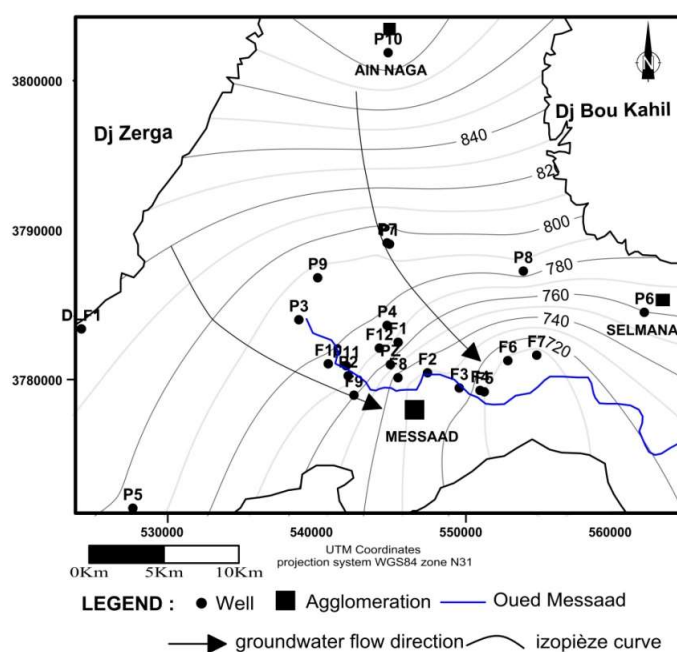


Fig.2. Piezometric map of the Barremian (July 2018).

2.3 Sampling and analysis (Fig. 02):

As part of this work, three water collection campaigns were conducted in November 2016, December 2017 (high water period) and July 2018 (low water period). These samples are carried out manually at the head of the drilling. The samples are taken from plastic bottles with a capacity of 1000 cm³. Three physico-chemical parameters (T°, pH, electrical conductivity) were measured in situ, immediately after sampling using a pH meter pHep

(HANNA), and a Delta OHM HD 3406.2 Field Conductivity Meter. The water analyses were carried out at the Water and Environment laboratory at the University of Tébessa. The methods used are: Volumetry for the elements (Ca^{2+} , Mg^{2+} , Cl^- , HCO_3^-), Atomic absorption spectrophotometry for the elements (Na^+ , K^+ , SO_4^{2-} , NO_3^- , NO_2^- , NH_4^+ , PO_4^{3-}). Data from water analyses conducted by the Algerian Water Company (AWC) in 2016 and 2017 were also used. For the reliability of the analysis results, the ion balance method was applied and an error of 5 % was accepted.

3. RESULTS AND DISCUSSIONS:

The results of the physico-chemical analysis of the water are summarized in the table 01.

The pH measurement of the study area water shows values that differ from well to well. In the high water period the pH varies between 7.2 and 7.6, whereas in the low water period the values vary between 7.4 and 7.8. The temperature of the collected water varies from 16 to 22.5°C, this variation in the temperature of the groundwater can be a function of the depth of the aquifer.

Conductivity values and chemical parameters are represented on maps using the Surfer 2013 software. The range of variation in conductivity during all companions varies from 550 $\mu\text{S}/\text{cm}$ to 8790.13 $\mu\text{S}/\text{cm}$. It should be noted that most samples have values greater than 2000 $\mu\text{S}/\text{cm}$. where the mapping of this parameter (Fig.03) shows that the major values are located in the downstream part of the catchment area near Oued Messaad. These high concentrations can be explained by a number of reasons, including the dissolution of salt-bearing formations during the groundwater flow from upstream to downstream. In addition, the Oued Messaad is the main waterway draining rainwater and domestic waste water, and all urban discharges; discharge a considerable polluting load.

In general, chemical mapping of the major elements studied in this work (Fig. 04,05,06) clearly shows that the areas near the Oued are very busy. In the majority of cases, high concentrations occur above the potability thresholds, where the mean values change in the same way as the conductivity for all measuring points. The distribution of major cations follows the following order of decay: $\text{Ca}^{2+} > \text{Na}^+ > \text{Mg}^{2+}$ and the distribution of major anions follows the following order of decay: $\text{SO}_4^{2-} > \text{Cl}^- > \text{HCO}_3^-$, this distribution confirms the predominance of calcium sulphate and calcium chloride facies on the global piper diagram (Fig.07), making it possible to say that the mineralization of water is essentially linked to SO_4^{2-} , Cl^- and Ca^{2+} ions, and evolved, from the 2nd to the 3rd stage of chemical evolution. Second, there are two other facies, calcium bicarbonate and sodium sulphate.

Table 1. Statistical variables and extreme values.

Elements (mg/l)	High Water Period				Low Water Period				
	Sta. WHO	Min	Max	Moy	Stan. devia.	Min	Max	Moy	Stan. devi.
HCO ₃ ⁻	250	225	401.6	293.07	44.14	218.2	389.50	284.1	42.81
SO ₄ ²⁻	250	36.1	2690	815.77	605.50	37.64	2804.9	850.6	631.3
Cl ⁻	250	6.80	1770	441.77	401.05	7.09	1752.5	453.1	403.9
Ca ²⁺	100	78.7	530.3	301.37	131.22	81.93	552.95	314.2	136.8
Mg ²⁺	50	9.60	285.5	80.97	78.45	9.31	276.86	78.52	76.07
Na ⁺	150	12.0	1252	249.89	257.00	12.51	1305.4	260.5	267.9
K ⁺	12	2.00	40	9.83	7.85	2.09	33.52	9.59	6.76
NO ₃ ⁻	50	0.34	55.90	12.59	13.53	0.3	51.16	9.8	11.84
NO ₂ ²⁻	0.1	0.01	0.04	0.02	0.01	-	-	-	-
NH ₄ ⁺	0.5	0.02	0.22	0.09	0.06	-	-	-	-
PO ₄ ³⁻		0.01	0.40	0.05	0.08	-	-	-	-
pH	6.5-9.5	7.2	7.60	7.3	0.12	7.4	7.8	7.60	0.12
EC _{μS/cm}	2500	550	8430	2791.9	1794.1	573.5	8790.1	2911	1870
T °C		16	22.5	18.3	1.31	16	21.4	18	1.32

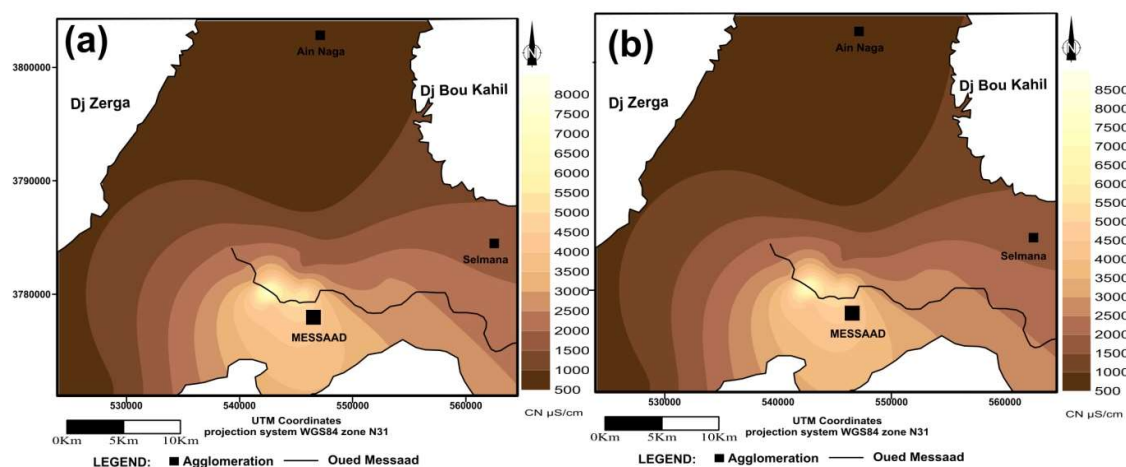


Fig.3. Conductivity maps. (a) High Water Period. (b) Low Water Period

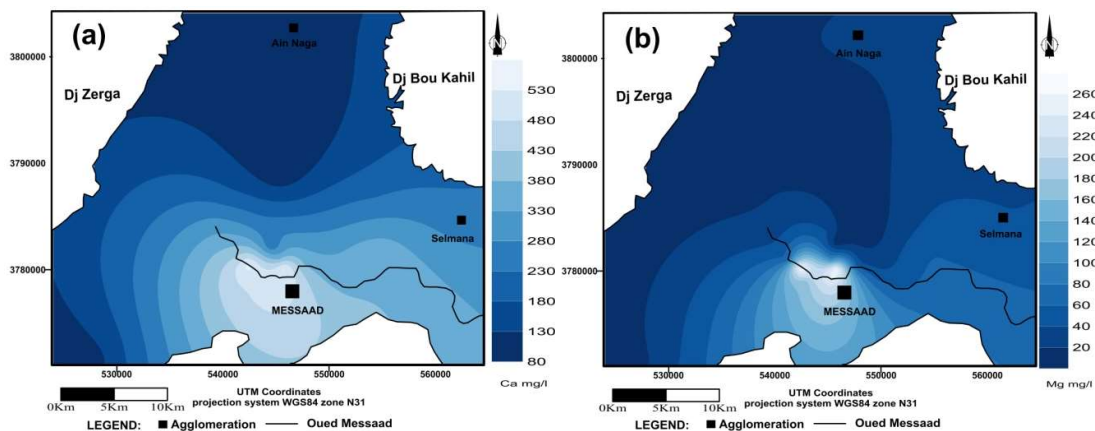


Fig.4. (a) calciums map. July 2018. (b) Magnesium map. July 2018

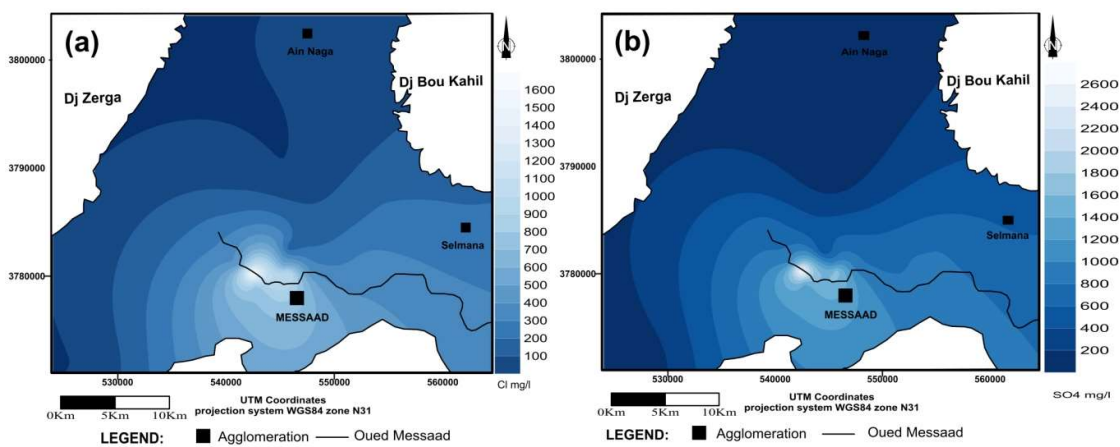


Fig.5. (a) Chloride map. July 2018. (b) Sulphate map. July 2018

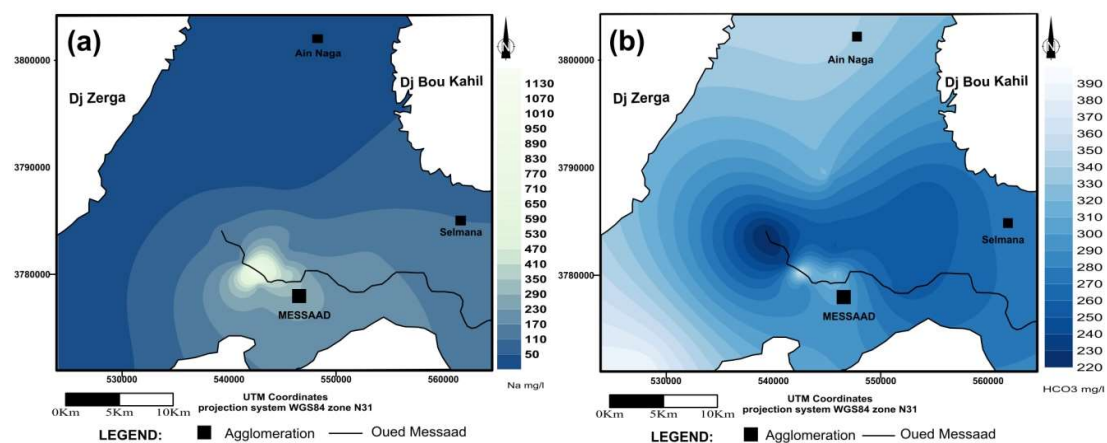


Fig.6. (a) sodiums map. July 2018. (b) bicarbonates map. July 2018

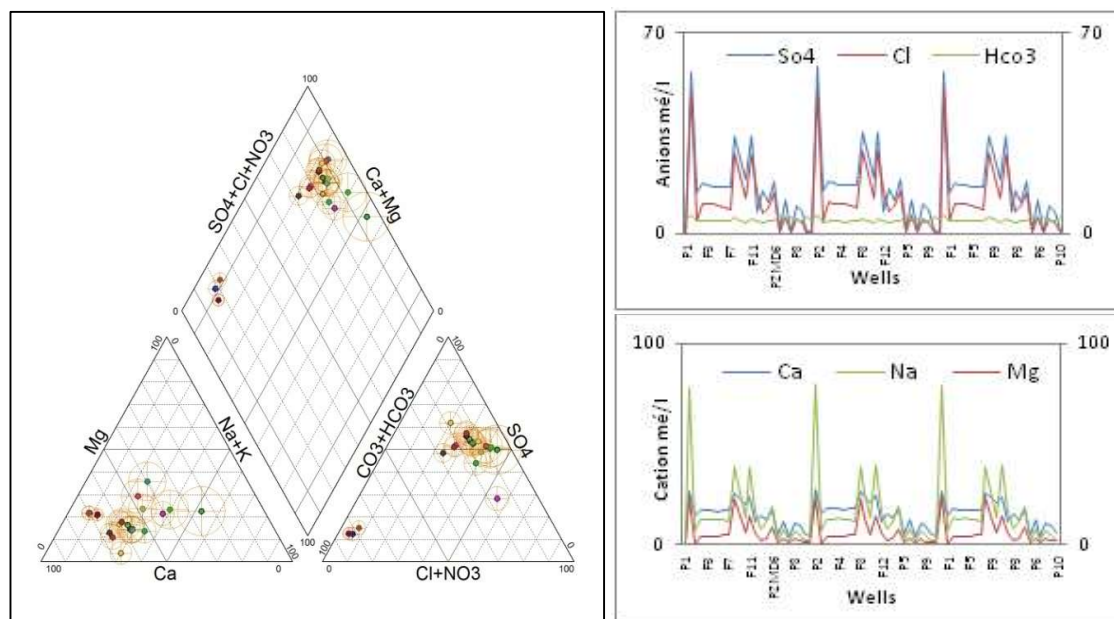


Fig.7. Piper diagram.

3.1. Principal Component Analysis (PCA)

This analysis was performed on a data table of 85 individuals and 14 variables which are: T°C, CE, pH, Ca²⁺, Mg²⁺, K⁺, Na⁺, NH₄⁺, HCO₃⁻, NO₃⁻, NO₂⁻, Cl⁻, SO₄²⁻, PO₄³⁻. We extended the analysis to three (3) factors and 75.70% of the variance could be expressed. The factors' own values are shown in Table 2.

Table 2. Own values and percentage of variance expressed.

Number	Own value	Percentage	Cumulative percentage
F1	7,0851	50,61	50,61
F2	2,0834	14,88	65,49
F3	1,4303	10,22	75,70

According to [12], for 85 individuals, the critical correlation coefficient is (0.43). Table (03) shows that there is a very strong correlation between EC electrical conductivity and sulphate (0.97), chloride (0.98), calcium (0.94), magnesium (0.90), sodium (0.93), and potassium (0.96). These correlations show that variations in dissolved ionic loads are entirely related to variations in the contents of these different ions. A strong correlation (0.77) between alkaline

earths (Ca^{2+} and Mg^{2+}). Ca^{2+} is strongly correlated with the ions SO_4^{2-} (0.97), Cl^- (0.88), K^+ (0.87), Na^+ (0.83), the ion Mg^{2+} is also well correlated with these ions Cl^- (0.94), SO_4^{2-} (0.96), Na^+ (0.79), K^+ (0.87) The latter are well correlated with each other, These bonds testify to the salinary influence on the water chemistry of the region. A strong correlation between NO_3^- and NH_4^+ (0.57), PO_4^{3-} (0.65), indicates that these parameters are put in solution by the same phenomenon. Low correlations are observed between the ion HCO_3^- and Mg^{2+} (0.15), EC (0.10), negative with SO_4^{2-} (-0.26), Cl^- (-0.11), Ca^{2+} (-0.36), Na^+ (-0.17), and K^+ (-0.01). There are also small negative correlations between pH and Ca^{2+} (-0.42), Mg^{2+} (-0.37), Na^+ (-0.38), K^+ (-0.35), Cl^- (-0.41), SO_4^{2-} (-0.42).

Table 3. Correlation matrix between variables

	Ca	Mg	Na	K	Cl	SO4	NO3	Hco	EC	pH	NO2	NH4	PO4	T
Ca	1													
Mg	0.77	1												
Na	0.83	0.78	1											
K	0.87	0.88	0.95	1										
Cl	0.88	0.92	0.94	0.95	1									
SO4	0.97	0.84	0.89	0.93	0.92	1								
NO3	-0.36	0.15	-0.17	-0.01	-0.11	-0.26	1							
Hco	0.12	-0.02	0.14	0.05	0.10	0.07	-0.25	1						
EC	0.94	0.90	0.93	0.96	0.98	0.97	-0.14	0.10	1					
pH	-0.42	-0.37	-0.38	-0.35	-0.41	-0.42	0.17	0.51	-0.40	1				
NO2	0.15	0.16	0.25	0.19	0.22	0.22	0.49	-0.17	0.20	-0.18	1			
NH4	-0.14	0.25	0.03	0.03	0.08	-0.01	0.57	-0.11	0.03	-0.03	0.46	1		
PO4	-0.32	-0.14	-0.22	-0.25	-0.22	-0.26	0.65	-0.13	-0.26	0.18	0.28	0.52	1	
T	0.41	0.45	0.54	0.57	0.53	0.44	0.07	-0.11	0.50	-0.26	0.32	-0.07	-0.28	1

Analysis of the factorial plane 1-2 shows that more than 65.49% of the total variance is expressed. (Fig. 08). The examination of plans shows that the parameters studied are divided almost into three groups. A group around the negative pole of the factor axis F1 and which

takes into account EC, SO_4^{2-} , Cl^- , Ca^{2+} , Na^+ , K^+ , Mg^{2+} , T° , so we can say that this axis presents a global mineralization of water, naturally these elements come from the dissolution of evaporative mineral-rich salt-bearing formations (Ca SO_4 , $\text{Ca SO}_4 \cdot 2\text{H}_2\text{O}$, Mg SO_4 , Na SO_4 , Ca Cl , Mg Cl and Na Cl), this axis represents the most charged water with conductivity values exceeding $2000 \mu\text{S}/\text{cm}$. In addition, negative correlations between pH and electrical conductivity, as well as between pH and the ions that are most involved in mineralization (SO_4^{2-} , Cl^- , Ca^{2+} , Na^+ , K^+ , Mg^{2+}) shows that the predominant redox mechanism over that of acid hydrolysis in the acquisition of these ions in the groundwater of the region [15].

The second F2 factor axis represents 14.88% of the variance and is determined by two poles. The first is formed by the bicarbonates HCO_3^- , this element has a very low correlation with the conductivity of water (0.10), so this element does not intervene in the determination of the mineralization of water, the spatial distribution of this element (Fig. 07 b) shows that the large values are located at the edges of the water table and diminished when one directs towards the Oued what can be interpreted by the supply of the water table by the carbonate formations of the Jurassic and Cretaceous, this pole represents the least loaded waters. The solution of the HCO_3^- ion in groundwater is controlled by the mechanism of acidic hydrolysis of carbonate minerals. The second pole of this axis is formed by polluting elements NO_3^- , NO_2^- , NH_4^+ and PO_4^{3-} . Nitrate values (NO_3^-) vary between [0.8 55.9] mg/l, which is the final stage of oxidation of organic nitrogen. The successive stages of nitrification are carried out through two families of bacteria mainly present in the soil: *Nitrosomonas* for nitritation (transformation of NH_4^+ into NO_2^-) and *Nitrobacter* for nitratation (transformation of NO_2^- to NO_3^-). Although the concentrations of these ions are below the guideline value for drinking water in WHO, the concentration of NO_3^- in wells P3 (30.1 mg/l) and P2 (55.9 mg/l) assumes contamination of well water. Indeed the proximity of these Oued wells and household waste depot could explain this high concentration of nitrates in the well water. The remaining water points showed nitrate concentrations below 20 mg/L. This grouping indicates that these parameters are solved by the same phenomenon. The probable natural source of nitrates is the decomposition of plant organic matter [14].

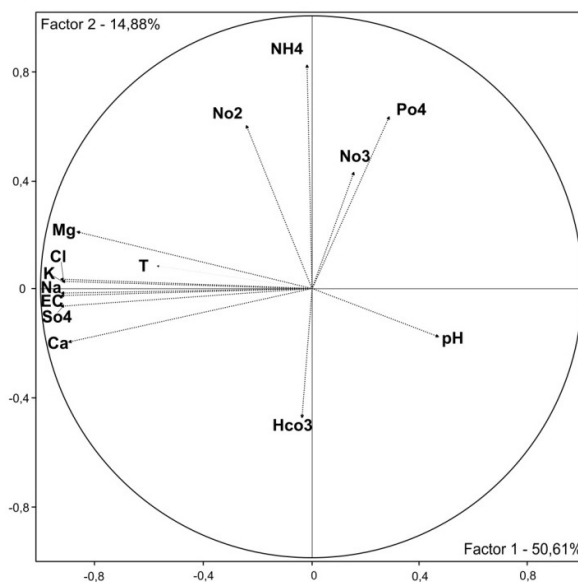


Fig.8. Space of factor plane variables F1 F2

3.2. Artificial Neuron Network (ANN):

Artificial neural networks, commonly known as ANN, are non-linear mathematical "black box" models able to establish relationships between the inputs and outputs of a system. Artificial neural networks have been basically inspired by the biological neural network consisting of a billion of interconnected neurons in the brain. The artificial network consists of a receiving layer through which information is entered to be processed, with or without the help of one or more hidden 'layers' containing one or more neurons and producing one or more output signals. The neurons are arranged in layers within the network such that the neurons of one layer are connected to those of the adjacent layer. The strength of these connections between two adjacent layers is called the weight and is equivalent to the strength of the signals in a biological neural network [18]. During the process of learning or training the weights of the interconnections are adjusted such until the inputs produce the desired output

In this work, a multi-layered Perceptron network was chosen as the model of the system. For the implementation of this model. Ca^{2+} , Mg^{2+} , Na^+ , K^+ , Cl^- , SO_4^{2-} , HCO_3^- , NO_3^- , were used as input vectors. The latter produces an output vector (output) which is electrical conductivity (EC). The MLP network can be represented by the following compact shape:

$$\{\text{EC}\} = \text{ANN} [\text{Ca}^{2+}, \text{Mg}^{2+}, \text{Na}^+, \text{K}^+, \text{Cl}^-, \text{SO}_4^{2-}, \text{HCO}_3^-, \text{NO}_3^-]$$

The data used in this study were previously standardized to be between 0 and 1 to facilitate the convergence of models during their learning. Where 25% of samples are used for the test, 50% for learning and 25% for validation. In the hidden layer, the transfer function used for each neuron is a tangent sigmoid, whose expression is:

$$F(S_j) = \frac{1}{1 + e^{-s_j}}$$

$F(S_j)$ is practically linear between 0 and 1.

The performance of the model can be evaluated through several indicators. Those used in this study are the mean relative error MRE, sum of the squared errors SSE, and the R^2 determination coefficient.

$$MRE = \frac{CE_i - \hat{CE}_i}{\hat{CE}_i}$$

$$SSE = \sum_{i=1}^n (CE_i - \hat{CE}_i)^2$$

$$R^2 = 1 - \frac{\sum_{i=1}^n (CE_i - \hat{CE}_i)^2}{\sum_{i=1}^n (CE_i - \overline{CE}_i)^2}$$

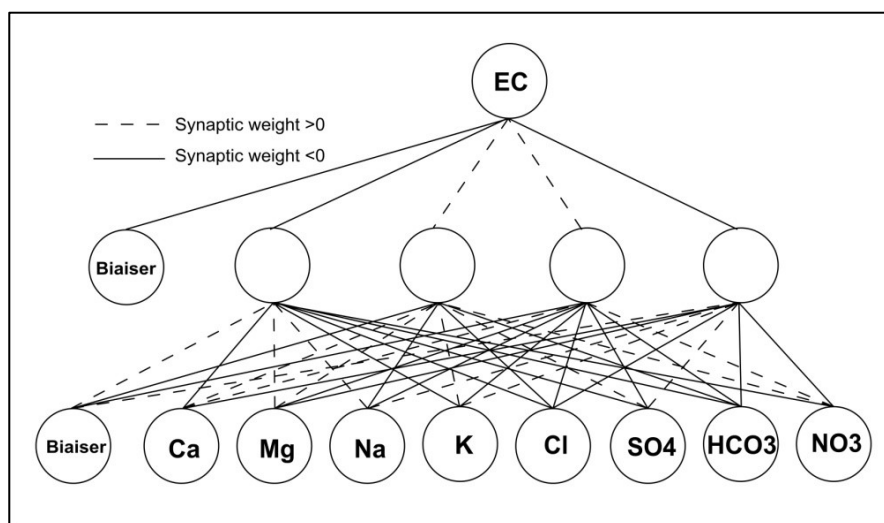
Where CE_i is the measured value of electrical conductivity, \hat{CE}_i is the conductivity calculated by the model. \overline{CE}_i is the mean of the measured conductivity and n the number of data in the calibration set. R^2 shows the change in the calculated or estimated electrical conductivity value by the linear regression.

To improve the performance of the model, several preliminary tests were carried out with different neural network architecture, where it was found that the best optimal model of the ANN is the three-layer MLP.

The results obtained by applying this method are summarized in Table 04. These are the neuronal models with the most optimal performance, according to the criteria for evaluating the performance of a model that must be greater than 80% for the correlation coefficient [6]. Examination of the table shows that the most appropriate architectural model is [8-4-1] (Fig.09).

Table 4. Criteria for assessing the performance of the ANN model for different architectures.

Architecteur	8-4-1	8-5-1	8-6-1
R²	0.989	0.968	0.943
LEARNING			
SSE	0.041	0.061	0.092
MRE	0.023	0.034	0.043
VERIFICATION			
SSE	0.008	0.014	0.045
MRE	0.017	0.035	0.054

**Fig.9.** Three-layer neural network architecture [8-4-1].

The [8-4-1] model shows an excellent agreement between measured and calculated conductivity with a correlation coefficient higher than 98%. The ANN sensitivity analysis of water quality variables in the verification phases shows that SO_4^{2-} , Cl^- , Ca^{2+} , Na^+ ions are the most important factors influencing electrical conductivity in groundwater (Fig.10).

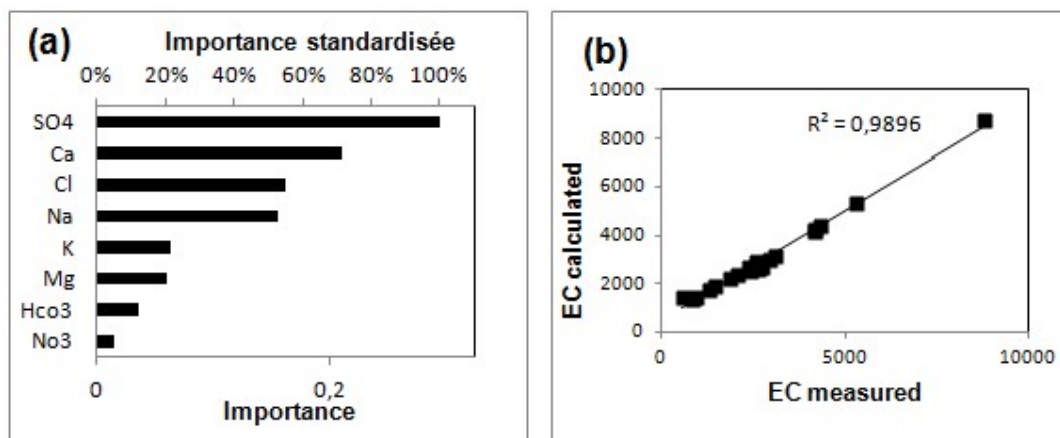


Fig.10. (a) Analysis of the importance of independent variables
(b) Correlation between calculated and measured conductivity.

3.3. Origin of major elements:

Ca^{2+} shows a very high variation in concentrations where 80% of the wells exceed the standards set by the WHO (standard deviation are relatively large 131) due to the dissolution of two different rocks which are; gypsum clays interspersed in the Barrémian formations and carbonate formations of the Jurassic and Cretaceous at the edge of the tablecloth. This is confirmed by Figure 11, which shows the evolution of calcium as a function of bicarbonates and sulphates, where 20% of all samples have a carbonate origin. Furthermore, the close R^2 correlation between the gypsum saturation index and the concentration $\text{Ca}^{2+} + \text{SO}_4^{2-}$ confirms that the majority of these ions have a common origin which would be the dissolution of the gypsum.

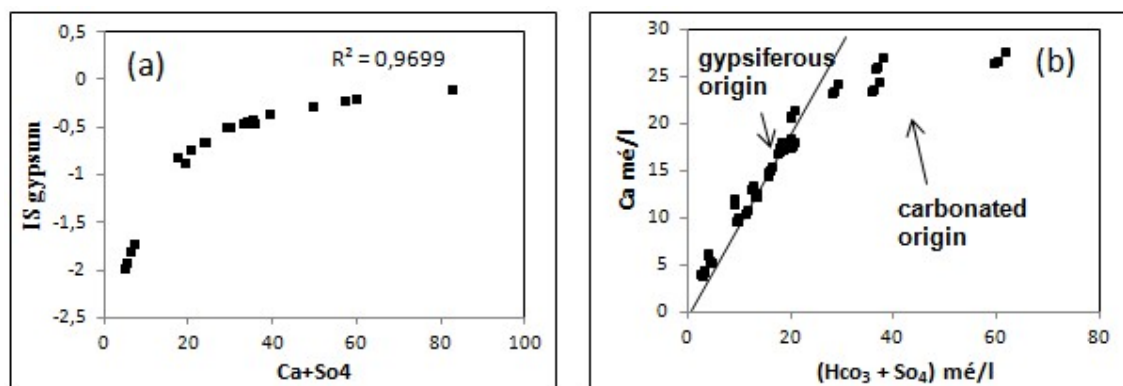


Fig.11. (a) Correlation of water saturation indices with gypsum as a function of $\text{Ca}^{2+} + \text{SO}_4^{2-}$, (R^2 : coefficient of determination). (b) Relationship $(\text{HCO}_3^- + \text{SO}_4^{2-})$ vs Ca^{2+} .

The SO_4^{2-} as the Ca^{2+} ion resulting from the dissolution of gypsum rocks according to the relation; $\text{CaSO}_4 \cdot 2\text{H}_2\text{O} = \text{Ca}^{2+} \text{SO}_4^{2-} + 2\text{H}_2\text{O}$. The large variation in concentrations of this element (standard deviation 605) could be explained by the lateral change in the faces of the Barremian formations from North-West to South-East [3], where the low values are located in the upstream part of the study area where the groundwater is at the beginning of its pathway, that is to say not yet too mineralized [8], the concentration becomes greater when one goes to the accumulation zone in the South-East, where the terrains become more clay [3].

Cl^- and Na^+ , have very high concentrations 80% of the wells exceed the standards set by the WHO and evaluate in the same way as SO_4^{2-} and Ca^{2+} . The origin of the Cl^- and Na^+ ions in the groundwater of the study area is the dissolution of the NaCl rich formations (clay and marl) this is confirmed by the important correlation between Cl^- and Na^+ (0,94) (Tab.03) and the close correlation between the halite saturation index and the concentration $\text{Cl}^- + \text{Na}^+$ (Fig.12 a). The concentrations of the SO_4^{2-} , Ca^{2+} , Cl^- and Na^+ elements which are the most important influencing the electrical conductivity are increasing according to the direction of flow of Nord-West to South-East, so the water gradually gets loaded by dissolving the formations rich in halite and gypsum (Fig. 12 b).

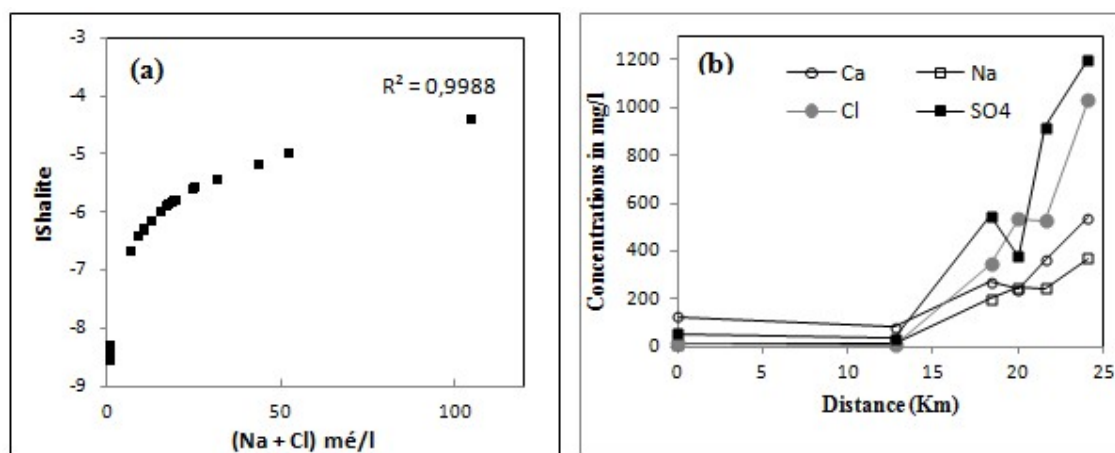


Fig.12. (a) Correlation of water saturation indices with halite as a function of $\text{Na}^+ + \text{Cl}^-$. (b) Evolution of elements SO_4^{2-} , Ca^{2+} , Cl^- and Na^+ next NW-SE groundwater flow direction.

K^+ results from the alteration of potash clay and the dissolution of chemical fertilizers used by farmers on the side of the Messaad Oued where concentrations of this ion reach its maximum 40mg/l.

Mg^{2+} has a small variation in the contents (standard deviation 78), with the exception of some wells near the Oued which have very high levels exceeding the potability standards, the

sewage in the Oued may be the cause, the low R^2 correlation between the dolomite saturation index and the concentration of Mg^{2+} (Fig. 13) confirms that the evolution of this ion content in the waters of the study area is linked to the dissolution of the evaporative minerals ($MgSO_4$, $MgCl$). This is confirmed only by the strong correlations that exist between these ions; Mg^{2+} vs SO_4^{2-} (0.84), Mg^{2+} vs Cl^- (0.92) (Tab. 03).

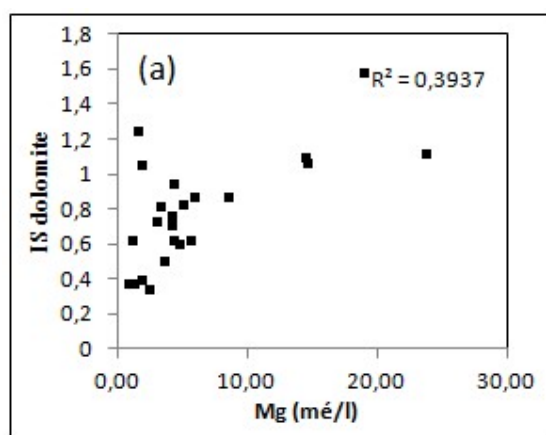


Fig.13. Correlation of water saturation indices with dolomite as a function of Mg^{+} .

However, the high values of these ions in wells P2, F8, F9 and F11, SO_4^{2-} [1267,5-2690] mg/l, Cl^- [710-1770] mg/l, Ca^{2+} [465-530] mg/l, Na^+ [265-1252] mg/l, with EC [4200-8430] $\mu s/cm$, assumes possible anthropogenic pollution of water from domestic wells, Indeed, these wells are very close to the Messaad Oued where the wastewater discharged directly into the Oued can infiltrate and contaminated the water table [9]. In addition, household waste is thrown directly into the Oued at random, this waste is exposed to rainwater and leads to the emergence of a liquid fraction called leachate (also called percolate) [5]. It can contaminate the water table and surface water [7].

4. CONCLUSION

The study area (Messaad plateau), it includes the Barrémien aquifer, which plays a very important role in the supply of drinking water and irrigation water. Our work on the quality of groundwater led to the following conclusions;

Almost all of the water points studied have very high conductivity values indicating high water mineralization, where most of the chemical parameters are higher than the WHO potability standard and sometimes well above the standard. The spatial distribution of the conductivity values and the various chemical parameters clearly reveal that the area near the

Messaad Oued is heavily laden, with a predominance of calcium sulphate and calcium chloride facies.

The statistical analyses used in this work allow us to know the main factors influencing the electrical conductivity and the acquisition mechanisms of the water mineralization and consequently the origin of the latter. The results obtained by the application of the PCA suggest that the increase in mineralization due essentially to the dissolution of the salt-bearing formations rich in evaporative minerals, the results of the PCA also showed that the predominant redox mechanism over that of acid hydrolysis in the acquisition of ions in the groundwater of the region. In addition, the construction of a hydro-chemical model based on networks of artificial neurons type Multi-Layer Perceptron (MLP) has shown that the best optimal model is the three-layer MLP. The [8-4-1] model has a strong correlation between calculated and measured conductivity (R^2 : 0.985), where the model's sensitivity analysis of water quality variables in verification phases shows that SO_4^{2-} , Ca^{2+} , Cl^- , Na^+ are the most important factors influencing the electrical conductivity of groundwater in the study area. The results achieved by the PCA and the ANN, therefore, the importance of the use of both methods in the investigation of the origin of the mineralization of groundwater and the precise determination of the main factors influencing its quality.

Groundwater chemistry is primarily related to the lithological nature of the Barremian aquifer in the study area. These are the salt-bearing formations that play an essential role in the mineralization of the water table. The graphs used in the study of the origin of the main major elements influencing electrical conductivity indicate that the ions Ca^{2+} and SO_4^{2-} come mainly from the dissolution of continuous gypsum in the Barremian formations, Ca^{2+} is also produced by the dissolution of the carbonate formation located especially in the North-West of the region, the ions Na^+ and Cl^- come from the dissolution of the continuous halite in the marls and clays especially in the South East of the region. These ions are the cause of the increased conductivity of the water, their contents increase according to the direction of flow from North-West to South-East.

5. REFERENCES

- [1] Aoun, S. *Gestion optimisée des ressources en eau d'une nappe côtière, Application à la plaine d'Annaba (Nord-Est Algérie)*. Thèse de doctorat, Univ. Lille, France, 2010, 211p.
- [2] Basseto, D., Guillemot, J. *Notice explicative de la carte géologique au 1/200.000 d'Aïn Rich*. Pub, Service Géol. Algérie, 1971, 74 p.

- [3] BERE GH (Bureau d'Etude & de Réalisation En Génie civil & Hydraulique). *Etude géophysique par prospection électrique dans la zone de Messaad wilaya de Djelfa*. 1^{ERE} phase, 2001, 35p.
- [4] Brou, A.L., Kouassi, L.K., Konan, S.K., Kouadio, A.Z., Konan, F.K., et Kamagate, B. *Modélisation Pluie-Débit à l'aide des Réseaux de Neurones Artificiels Multicouches sur le Bassin Versant du Fleuve Cavally à la station d'Ity (Zouan-Hounien, Côte d'Ivoire)*. Journal International Sciences et Technique de l'Eau et de l'Environnement, 2017, 2(5):19-23.
- [5] Chofqi, A. *Mise en évidence des mécanismes de contamination des eaux souterraines par les lixiviats d'une décharge incontrôlée (El Jadida, Maroc) : géologie, hydrogéologie, géoélectrique, géochimie et épidémiologie*. Thèse de doctorat, Univ. d'El Jadida, Maroc, 2004, 250 p.
- [6] Doukouré, C. *Application de la modélisation neuronale à l'évaluation du risque de contamination des eaux souterraines par les pesticides*. Thèse de doctorat, Univ. Québec, Canada, 2007, 182p.
- [7] Emilien, B. *Évolution de l'impact environnemental de lixiviats d'ordures ménagères sur les eaux superficielles et souterraines, approche hydrobiologique et hydrogéologique. Site d'étude: décharge d'Étuefont (Territoire de Belfort -France)*.Thèse de doctorat, Univ. Franche-Comté, France, 2008, 248p.
- [8] Gouaidia, L. *Influence de la lithologie et des conditions climatiques sur la variation des paramètres physico –chimiques des eaux d'une nappe en zone semi-aride, cas de la nappe de Meskiana Nord-Est Algérien*. Thèse de doctorat, Univ. Annaba, Algérie, 2008, 199p.
- [9] Henri, J.S. *Groundwater Pollution (Proceedings of the Moscow Symposium)*. IAHS-AISH, 1971, Publ. No.103, 7p.
- [10] Hidouche, N. *Synthèse des études hydrogéologiques de la partie Ouest du bassin versant du chott melrhir (wilaya de Laghouat et Djelfa)*, ANRH, Algérie, 2003, 46p.
- [11] HYDROG (Bureau d'études et de réalisations). *Etude géologique et hydrogéologique des régions de Deldoul et Sed-Rahal (Messaad-wilaya de Djelfa)*, La générale des concessions agricoles, Algérie, 2000, 66p.
- [12] Mangin, A. *Contribution à l'étude hydrodynamique des aquifères karstiques. Concepts méthodologiques adoptés. Systèmes karstiques étudiés*. Annales de Spéléologie, 1974, pp. 294, 495, et 601.
- [13] Manssouri, T., Sahbi, H., Manssouri, I., et Boudad, B. *Utilisation d'un modèle hybride base sur la RLMS et les RNA-PMC pour la prédiction des paramètres indicateurs de la*

qualité des eaux souterraines, Cas de la nappe de Souss-Massa- Maroc, European Scientific Journal, 2015, 11(18): 36-46.

[14] Matini, L., Moutou, J.M., et Kongo-Mantono, M.S. *Evaluation hydro-chimique des eaux souterraines en milieu urbain au Sud-Ouest de Brazzaville*. Congo. Afrique SCIENCE, Revue Internationale des Sciences et Technologie, 2009, 5(1):82-98.

[15] McMahon, P.B., Chapelle, F.H., and Bradley, P.M. *Evolution of Redox Processes in Groundwater*. ACS Symposium Series. American Chemical Society, 2011, 1071(26):581-597.

[16] Pouget, M. *Cartographie des zones arides, géomorphologie, pédologie, groupements végétaux, aptitudes du milieu a la mise en valeur. Région de Messaad-Aïn El Ibel (Algérie)*. Notice explicative No 67, ORSTOM, Paris, 1977, 101p.

[17] Solages, S., Rey, E. *Etude hydrogéologique en vue de l'implantation de 2 forages de reconnaissance dans les régions d'Aïn el lbel et Aïn el Hadjel*, Etude No. 20/11, DEMRH, Alger, 1971, 13 p.

[18] Tanty, R., Desmukh, T. *Application of Artificial Neural Network in Hydrology*. A Review. International Journal of Engineering Research & Technology, 2015, 4(6):184-188.

How to cite this article:

Rahmani B E, Baali F, Fehdi C. Using pca and ann in the explanation of groundwater chemism. Case of the messaad plateau. South algerian steppe region. J. Fundam. Appl. Sci., 2022, 14(1), 88-106.